IV Escola de Primavera de Transição e Turbulência
Universidade Federal do Rio Grande do Sul
Pontifícia Universidade Católica do Rio Grande do Sul
Porto Alegre, RS, 27 de setembro a 1º de outubro de 2004

Numerical Simulation of Flows Over a Shallow Open Cavity With Moving Bottom Using the Immersed Boundary Method

Juliano Marcelo de Arruda
Federal University of Uberlândia
Mechanical Engineering College
Campus Santa Mônica, 38400-902, Uberlândia, MG, Brasil
jmarruda@mecanica.ufu.br

Ana Lúcia Fernandes de Lima e Silva
Federal University of Uberlândia
Mechanical Engineering College
Campus Santa Mônica, 38400-902, Uberlândia, MG, Brasil
alfsilva@mecanica.ufu.br

Alexandre Megiorin Roma
Institute of Mathematics and Statistics
University of São Paulo
Cidade Universitária, 05315-970, São Paulo, Brasil
roma@ime.usp.br

Aristeu da Silveira Neto
Federal University of Uberlândia
Mechanical Engineering College Campus Santa Mônica, 38400-902, Uberlândia, MG, Brasil
aristeus@mecanica.ufu.br

Abstract. *The numerical simulation of flows over a shallow open cavity with moving boundary is performed using the Immersed Boundary Method (IBM). The IBM with the Virtual Physical Model (VPM) has been used to simulate external flows in presence of complex geometry such as cylinders by Lima e Silva et al., 2003. In the present work this methodology is adapted and used to simulate internal and forced flows. The cavity walls were modeled by the VPM, which is based on the solution of the Navier-Stokes equations to compute the Lagrangean force field. This force field is distributed and applied to the flow in the neighboring wall grids. This way, the cavity walls are modeled in a virtual manner inside a rectangular calculation domain. Numerical results of the present work are compared with experimental and numerical results of others authors.*

Key-words: immersed boundary methodology, virtual physical model, shallow open cavity, moving boundaries.

1. Introduction

The Immersed Boundary Method (IBM) was developed at the early 70´s in order to simulate flows in the human hearth, with the goal of optimize artificial valves design (Peskin, 1972, 1977). Others Computational Fluid Dynamics (CFD) problems were also simulated with this methodology, such as the modeling of biofilm processes (Dilon *et al*., 1996), the model of aquatic animal locomotion (Fauci and Peskin, 1998), multi-fluid flows (Unverdi and Tryggvason, 1992) and flows over cylinders (Goldstein *et al*., 1993; Saiki and Biringen, 1996; Lima e Silva *et al*., 2003).

The main idea of IBM is to solve, numerically, the flow for a whole Eulerian domain, while the bodies present in the flow are modeled by a Lagrangian mesh. The bodies forces, also known as interfacial force, is computed by the Lagrangian mesh, and is interpolated to the Eulerian mesh. Many authors have been looked for alternative ways to compute that interfacial force. Unverdi and Tryggvason (1992) proposed the Front-tracking Method, where two phase flows are modeled using only the physical and geometrical parameters and interfacial stress are used to compute the force field. Goldstein *et al*. (1993) proposed the Virtual Boundary Formulation, where the sum of inertial forces of the body is used to compute the interfacial force. Lima e Silva *et al*. (2003) developed the Virtual Physical Model (VPM) to compute the interfacial force using the Navier-Stokes equations applied to the Lagrangian mesh. These authors modeled flows over isolated cylinders, cylinders disposed in tandem, cylinders side-by-side and airfoils. The VPM was also used by Arruda *et al*., (2003) to model channel flows and lid driven cavities and by Arruda *et al*. (2004) to model shallow open cavities.

The IBM, coupled with the VPM, are used in the present work to model an shallow open cavity with a moving bottom. The cavity is considered initially as an square, then its bottom moves up, and it becomes a rectangular cavity. Finally, the bottom moves down, and the cavity takes over its originally shape. The results are confronted with the experimental results of Sinha *et al*. (1982) and with the numerical results of Arruda *et al*. (2004).

2. Mathematic Model

2.1. Immersed Boundary Method

The main idea of the IBM is to use a regular Eulerian mesh, for the fluid dynamics simulation, coupled with a Lagrangean mesh that represents the immersed boundary, as can be seen in Fig. (1). There is an interaction among the Eulerian mesh, which is independent from the boundary geometry, and the Lagrangean mesh. The immersed boundary exerts a singular force in the fluid, $\vec{F}_k$.

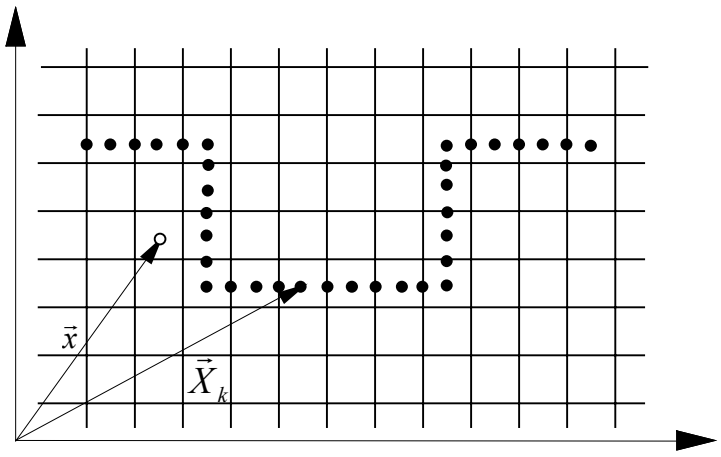

Figure 1. Immersed Boundary Method – Eulerian mesh and Lagrangean mesh.

It is considered incompressible and isothermal flows of Newtonian fluids for the entire Eulerian domain, and the governing equations are the mass and the momentum conservation equations:

$$\vec{\nabla}\cdot\vec{V} = 0\,, \tag{1}$$

$$\rho\left[\frac{\partial\vec{V}}{\partial t} + \left(\vec{V}\cdot\vec{\nabla}\right)\cdot\vec{V}\right] = -\vec{\nabla}p + \vec{\nabla}\cdot\left[\mu\left(\vec{\nabla}\cdot\vec{V} + \vec{\nabla}^T\cdot\vec{V}\right)\right] + \vec{f}\,. \tag{2}$$

Since the flow may be at turbulence transition, or even in turbulence regime, the Large Eddy Simulation, coupled with the Smagorinsky sub-grid scale model, is used in order to completely model the flow (Silveira-Neto,1991).Thus Eqs. (1) e (2) should be rewrite as:

$$\vec{\nabla}\cdot\overline{\vec{V}} = 0\,, \tag{3}$$

$$\rho\left[\frac{\partial\overline{\vec{V}}}{\partial t} + \vec{\nabla}\cdot\left(\overline{\vec{V}}\,\overline{\vec{V}}\right)\right] = -\vec{\nabla}\,\overline{p} + \vec{\nabla}\cdot\left[\mu_{ef}\left(\vec{\nabla}\overline{\vec{V}} + \vec{\nabla}^T\,\overline{\vec{V}}\right)\right] + \overline{\vec{f}}\,, \tag{4}$$

where $\bar{}$ symbol indicates a filtered variable and μ_{ef} is the effectiveness viscosity, which is:

$$\mu_{ef} = \mu + \mu_t\,, \tag{5}$$

where μ_t is the eddy-viscosity, and μ is the molecular viscosity. The eddy-viscosity , μ_t , is given by

$$\mu_t = (C_s l)^2\left(\overline{S}_{ij}\overline{S}_{ij}\right)^{1/2}. \tag{6}$$

C_s is the Smagorinsky constant, empirically determined, C_s=0.18, l is the Smagorinsky sub-grid scale length, and S_{ij} the strain rate stress.

The force term, $\vec{f}$, is computed by the Lagrangian force density, $\vec{F}_k$, and a Delta of Dirac function, and is given by:

$$\vec{f}(\vec{x}) = \int_{\Omega} \vec{F}(\vec{x}_k)\,\delta(\vec{x}-\vec{x}_k)\,d\vec{x}_k . \tag{7}$$

The Delta of Dirac is replaced by a distribution function D_{ij}, given by

$$\vec{f}_{ij} = \sum D_{ij}(\vec{x}-\vec{x}_k)\vec{F}_k(\vec{x}_k)\Delta s^2(\vec{x}_k), \tag{8}$$

where $\Delta s(\vec{x}_k)$ is distance between the Lagrangian nodes, as can be seen in Fig. (2). The k index is relative to the Lagrangean nodes, and the i and j index are relative to the Eulerian nodes.

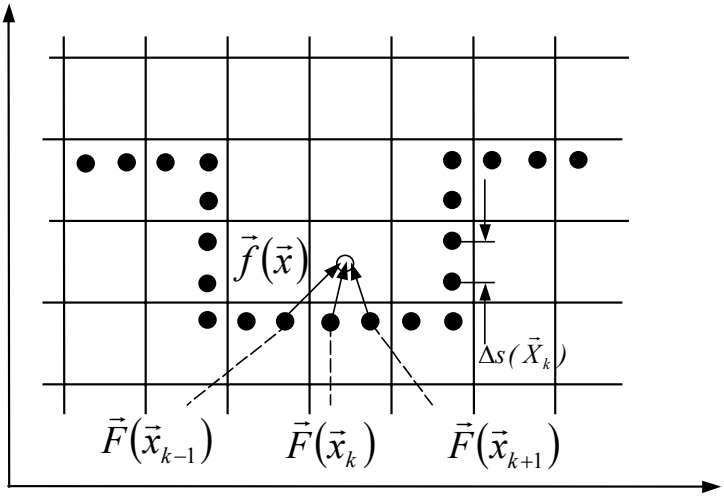

Figure 2. Immersed Boundary Method – Lagrangean force distribution process.

The distribution function used in the present work was proposed by Juric (1996), and it has the proprieties of a Gaussian Function. This function is defined as

$$D_{ij}(\vec{x}_k) = \frac{f\left[(\vec{x}_k - \vec{x}_i)/h\right] f\left[(\vec{y}_k - \vec{y}_j)/h\right]}{h^2}, \tag{9}$$

with

$$f(r) = \begin{cases} f_1(r) \;\; se \;\; \|r\| < 1 \\ \frac{1}{2} - f_1(2 - \|r\|) \;\; se \;\; 1 \le \|r\| \le 2 \\ 0 \;\; se \;\; \|r\| > 2 \end{cases} \tag{10}$$

where

$$f_1(r) = \frac{3 - 2\|r\| + \sqrt{1 + 4\|r\| - 4\|r\|^2}}{8}, \tag{11}$$

r being $(x_k - x_i)/h$ in the x direction, or $(y_k - y_i)/h$ in the y direction, and h is the Eulerian mesh step.

2.2. Virtual Physical Model-VPM

The Lagrangean Force density $\vec{F}_k$ is computed by the Navier-Stokes terms applied over the Lagrangean nodes, defined as:

$$\vec{F}(\vec{x}_k) = \vec{F}_a(\vec{x}_k) + \vec{F}_i(\vec{x}_k) + \vec{F}_v(\vec{x}_k) + \vec{F}_p(\vec{x}_k), \tag{12}$$

where,

$$\vec{F}_a(\vec{x}_k) = \rho \frac{\partial \vec{V}(\vec{x}_k)}{\partial t}, \tag{13}$$

$$\vec{F}_i(\vec{x}_k) = \rho(\vec{V}\ \vec{\nabla})\vec{V}(\vec{x}_k), \tag{14}$$

$$\vec{F}_v(\vec{x}_k) = -\mu \nabla^2 \vec{V}(\vec{x}_k), \tag{15}$$

$$\vec{F}_p(\vec{x}_k) = \vec{\nabla}\, p(\vec{x}_k), \tag{16}$$

are the acceleration force, the inertial force, the viscous force and the pressure force respectively. These terms are calculated over the boundary, using the velocity and pressure fields. It should be noted that, over the boundary, the fluid velocity, $\vec{V}_{fk}(\vec{x})$, and the boundary velocity, $\vec{V}_k(\vec{x}_k)$, must be equal, satisfying the non-slip condition. Once the velocity and pressure fields are obtained, from the Eqs. (3) and (4), they are interpolated to obtain the terms presented in Eqs. (13)-(16). This interpolation is performed using four auxiliary points, which can be seen in Fig. (3). In this figure the auxiliary points are shown for two different Lagrangean points, k_1 e k_2.

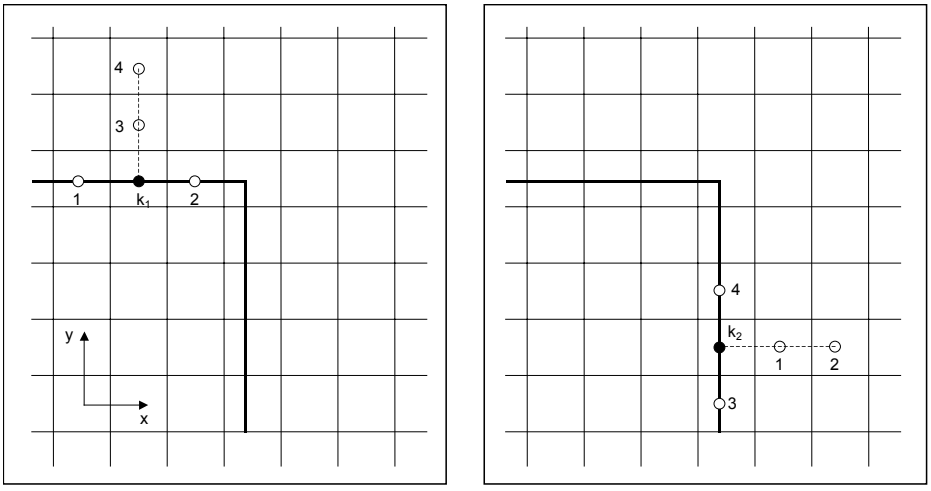

Figure 3. Scheme for position of the auxiliary points 1, 2, 3 and 4 during the interpolation process of the velocity and pressure.

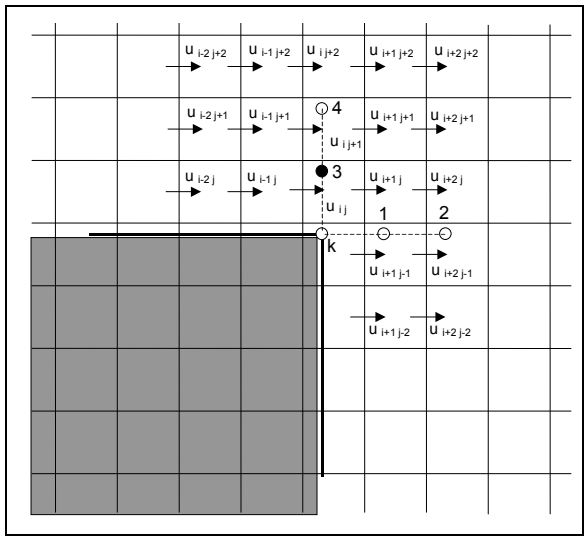

Figure 4. Interpolation scheme of the horizontal velocity for the point 3.

Figure (4) shows the velocity and pressure interpolation process to the auxiliary points (example for the point 3 in the scheme). It must be noted that the four auxiliary points are located in the internal region of the boundary. This condition is reached by the Indicator Function, proposed by Unverdi and Tryggvason (1992), which allows to identify

regions of fluids with distinct properties. Further details of the interpolation process can be seen in Lima e Silva et al. (2003) and Arruda (2004).

3. Numerical Method

The governing equations were spatially discretized by the second order finite central difference method, and temporally by the second order Runge-Kutta scheme.

The pressure-velocity coupling (*P-V*) was solved by the Fractional Step Method (Armfield e Street, 1999), which allows to reach the mass conservation with just one numerical interaction.

The linear system resulting from the *P-V* coupling are solved by the *Modified Strongly Implicit Procedure – MSI* (Schneider e Zedan, 1981).

4. Results

The goal of this work was to evaluate the coupling *IBM-VPM* for the case of modeling internal forced flows between stationary or moving walls. Once the shallow open cavity was already successfully simulated (Arruda *et al*., 2004), it seems natural the implementation of a moving bottom in such cavity. The physical model for the moving bottom cavity is presented in Fig. (5).

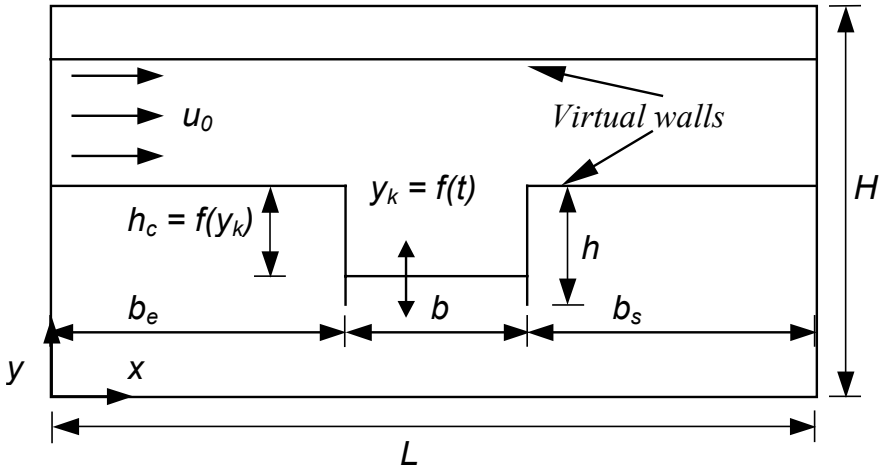

Figure 5. Physical model for the shallow open cavity with moving boundary.

Initially a flow over a shallow open cavity with aspect ratio of h_c/h = 1.0 was simulated. After the flow was established, the bottom was displaced up, gradually, to the aspect ratio h_c/h = 0.5. The flow was simulated during the bottom displacement. We emphasize that it is a domain of variable geometry that is simulated using a fixed Eulerian mesh and a moving Lagrangean mesh. After the flow is established, the bottom moves down to the initial position, coming back to a cavity of aspect ratio h_c/h = 1.0. Since the cavity height changes, the Reynolds number also changes, from *Re* = 2648, to *Re* = 1324, and coming back to *Re* = 2648. The flow conditions for this simulation are presented in Tabs. 1 and 2. The Reynolds is defined as a function of h_c The Eulerian mesh has 200x100 points and the Lagrangean mesh has 1000 points.

Table 1. Unchanged parameters values.

h [m]	b [m]	b_e [m]	b_s [m]	u_0 [m/s]	L [m]	H [m]
0.025	1h	3h	4h	1.8	8h	4h

Table 2. Variable parameters values.

Re	h_c [m]
2648	1h
1324	0.5h

It was imposed to all Lagrangean points of the bottom wall a velocity, which is function of time. Initially, this velocity is positive, when the bottom is moving up, and posteriori the velocity is negative, when the bottom moves down. The bottom displacement is a function of this velocity, and is given by:

$$y_k = y_k + v_k \Delta t \,, \tag{17}$$

where y_k is the bottom wall position, v_k the bottom wall velocity e Δt is the time step, which is the same time step used for the flow simulation.

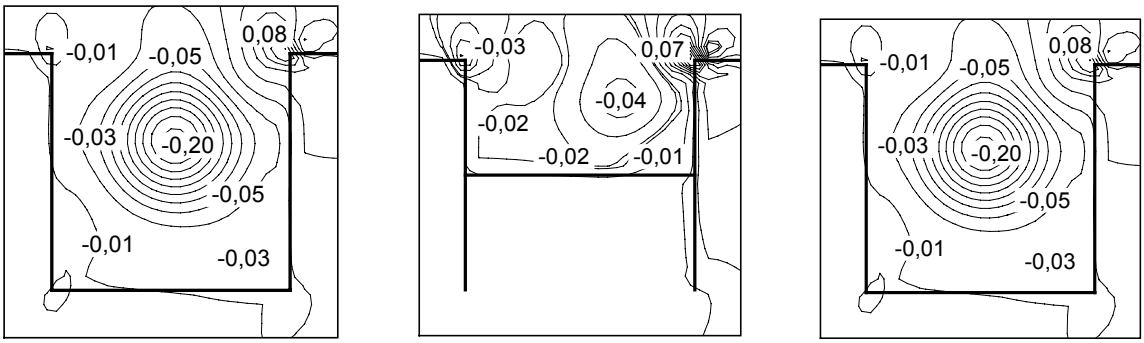

(a) (b) (c)

Figure 6. Pressure contours at the cavity region: (a) Re = 2648, h_c/h = 1.0, (b) Re = 1324, h_c/h = 0.5 and (c) Re = 2648, h_c/h = 1.0.

Figure (6) shows the pressure contours for three different times. First the bottom wall moves of the inferior position, reaches the superior position (middle of the cavity) and comes back to the inferior position, completing a cycle. It should be noted that the results strongly agree with those of Arruda *et al*., (2004), determined for the simulation of a cavity with stationary boundaries. The pressure distribution inside the shallow open cavity with moving boundary, obtained in the present work, was compared with the shallow open cavity for stationary walls, Arruda *et al*., (2004). Figure (7) shows that these results are very close. Nevertheless, there is a difference when these results are compared with the experimental results of Sinha *et al*. (1982). This difference may due to the fact that the Sinha results are the time average for the pressure, while the results of the present work are instantaneous results.

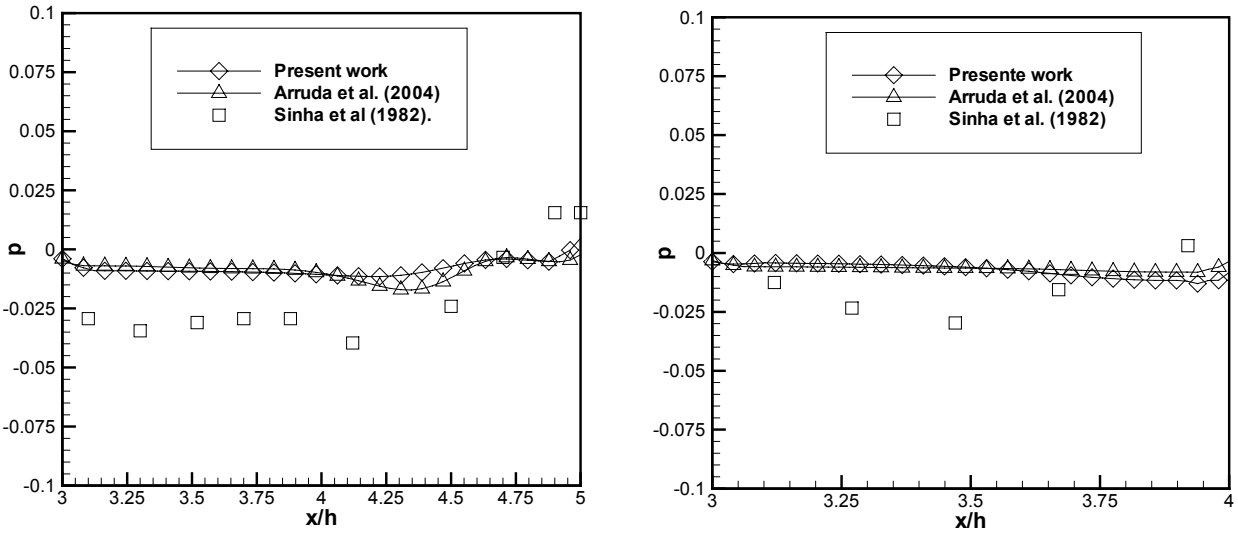

(a) (b)

Figure 7. Pressure distribution: (a) Re = 1324, h_c/h = 0.5 and (b) Re = 2648, h_c/h = 1.0.

The comparison between the results of the shallow open cavity with moving boundary and the results of the shallow open cavity with stationary walls are presented in Fig. (8). This figure shows the velocity profiles at several positions of the cavity. It may be observed that, in both cases, Re = 2648 and Re = 1324, small differences are present in the velocity profiles. These differences are larger next the cavity geometric center, and smaller near the cavity walls. They may exist because it is compared instantaneous values, instead of mean values. The recirculating cells may be oscillating inside the cavity. Despite of that the results are very close.

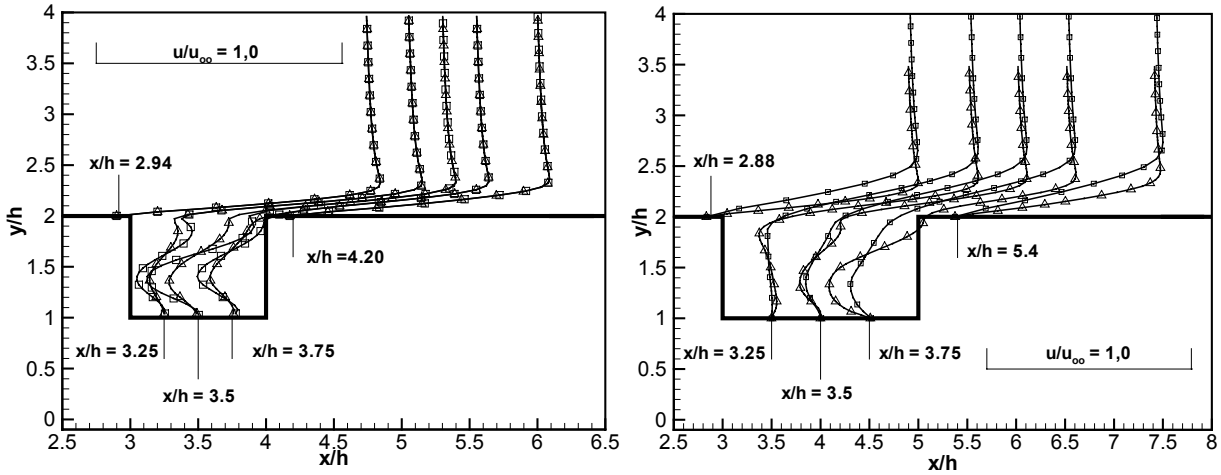

(a) (b)

Figure 8. Horizontal velocity profiles: (a) Re = 2648, h_c/h = 1.0 e (b) Re = 1324, h_c/h = 0.5. □ present work and Δ Arruda *et al*. (2004).

Figure (9) presents the streamlines details. Figure (9.a) shows the streamlines at the moment in which the bottom wall is in its upper position. The internal recirculating cells are close to the recirculating cells of the cavity with static bottom. The external recirculating cells are formed by induction of the bottom wall moving up.

Figure (9.b) shows the internal cavity flow, with the presence of a primary recirculating cell, and two smaller ones at the lower corners, the biggest next to the right wall, and the smallest next to the left wall. The external flow was developed due to the force field. The external field develops in a such way that the no-slip condition is naturally established.

(a) (b)

Figure 9. Streamlines: (a) Re = 1324, h_c/h = 0.5 and (b) Re = 2648, h_c/h = 1.0.

As already mentioned, the Eulerian domain above the Lagrangean mesh is a region of spontaneous flows, formed due the no-slip condition and is not a region of interest. The bottom wall displacement creates another cavity, occupied by recirculating structures naturally formed. When the bottom wall comes back to the initial position, these recirculating structures of the external flow vanish. This is an important fact, that shows a complete interaction among the Eulerian and the Lagrangean meshes and the Lagrangean mesh influence over the entire Eulerian domain during the whole simulation.

The shape and the length of the recirculating structures for the shallow open cavity with moving boundary and for the shallow open cavity (Arruda *et al*., 2004) were compared. Table 3 presents the recirculating structures center location and Tab. 4 presents the recirculating structures length. These tables show that some recirculating structures were displaced and/or compacted in some directions. The differences noted in both cases is due to the fact that the computations are performed with instantaneous velocity fields, despite the mean velocity fields.

Table 3. Recirculating structures center location.

Case	Primary vortex		Left vortex		Right vortex	
	x [m]	y [m]	x [m]	y [m]	x [m]	y [m]
Re = 1324 Arruda *et al* (2003)	0.54	0.64	0.06	0.13	0.82	0.16
Re = 1324 Present work	0.52	0.64	0.15	0.14	0.81	0.17
Re = 2648 Arruda *et al* (2003)	0.71	0.60	0.18	0.51	0.93	0.13
Re = 2648 Present work	0.68	0.66	0.13	0.42	0.94	0.16

Table 4. Recirculating structures length.

Caso	Left vortex		Up vortex		Rigth vortex	
	l_x [m]	l_y [m]	l_x [m]	l_y [m]	l_x [m]	l_y [m]
Re = 2648 Arruda *et al* (2003)	0.0066	0.0048	—	—	0.0101	0.0118
Re = 2648 Present work	0.0091	0.0056	—	—	0.0133	0.0101
Re = 1324 Arruda *et al* (2003)	0.0264	0.0197	0.0199	0.0074	0.0055	0.0063
Re = 1324 Present work	0.0081	0.0125	—	—	0.004	0.0306

It was also observed differences in the vorticity contours, with relevant increases, mainly at the central regions, as can be seen in Fig. (10), which presents the vorticity contours.

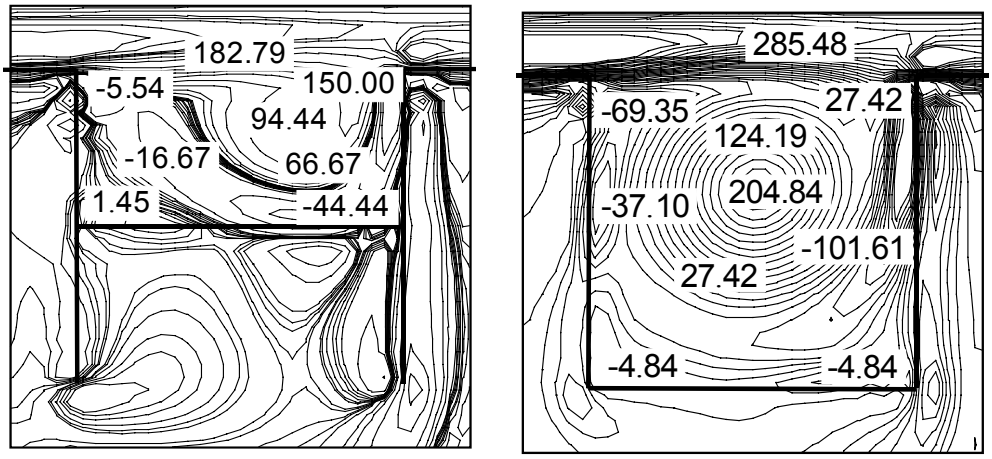

(a) (b)

Figure 10. Shallow open cavity with moving boundary – Vorticity contours: (a) *Re* = 1324, h_c/h = 0.5; (b) *Re* = 2648, h_c/h = 1.0.

5. Conclusions

A shallow open cavity with moving boundary was simulated using the Immersed Boundary Method (*IBM*) and the Virtual Physical Model (*VPM*). The coupling *IBM-VPM* shows to be efficient to model an internal forced flow and a moving boundary perpendicularly to the flow. The model (*VPM*) was able to capture the present recirculating structures in the cavity flow, and the results obtained show that the model is a promising tool to simulate internal forced flows with complex and mobile geometries.

6. Acknowledgments

The authors acknowledge the CNPq for the financial support and the Mechanical Engineering School-UFU for the technical support.

7. References

Armfield, S., e Street, R., 1999, "The Fractional-Step Method for the Navier-Stokes on Staggered Grids: The Accuracy of three Variations". NOTE. Journal of computational Physics, **153**, pp. 660-665.

Arruda, J. M., Lima e Silva, A. L. F., Silveira Neto, A. e Roma, A. M., 2003, "Numerical Simulation of Flows in a Presence of Moving Boundaries Using the Immersed Boundary Method", Proceedings of the 17th International Congress of Mechanical Engineering, São Paulo, SP, Brasil.

Arruda, J. M., 2004, "Modelagem Matemática de Escoamentos Internos Forçados Utilizando o Método da Fronteira Imersa e o Modelo Físico Virtual", Tese de Doutorado, Universidade Federal de Uberlândia, Uberlândia, MG, Brasil.

Arruda, J. M., Lima e Silva, A. L. F., Silveira Neto, A. e Roma, A. M., 2004, "Simulação Numérica de Escoamentos sobre Cavidades Abertas Rasas Utilizando o Método da Fronteira Imersa", Proceedings of the ETT 2004 – IV Escola da Primavera de Transição e Turbulência, Porto Alegre, RS, Brasil.

Dillon, R. et al., 1996, "Modeling Biofilm Processes Using the Immersed Boundary Method", Journal of. Computational Physics, **129**, pp. 57-73.

Fauci, L. J. e Peskin, C. S., 1988, "A Computational Model of Aquatic Animal Locomotion", Journal of. Computational Physics, **77**, pp. 85-108.

Goldstein, D., Hadler, R. e Sirovich, L., 1993, "Modeling a no-slip flow boundary with an external force field", Journal of Computational Physics, **105**, 354.

Juric, D., 1996, "Computation of Phase Change", Ph.D. Thesis, Mechanical Engineering, University of Michigan.

Lima e Silva, A. L. F., Silveira Neto, A. e Damasceno, J. J. R., 2003, "Numerical Simulation of Two Dimensional Flow over a Circular Cylinder using the Immersed Boundary method", Journal of. Computational Physics, **189**, pp. 351-370.

Peskin, C.S., 1972, "Flow Patterns Around Heart Valves: A Numerical Method", Journal of. Computational Physics, **10**, pp. 252-271.

Peskin, C.S., 1977, "Numerical Analysis of Blood Flow in the Heart", Journal of. Computational Physics, **25**, pp. 220-252.

Saiki, E. M. e Biringen, S., 1996, "Numerical Simulation of a Cylinder in Uniform Flow: Application of Virtual Boundary Method", Journal of. Computational Physics, **123**, pp. 450-465.

Schneider, G. E., e Zedan, M., 1981, "A Modified Strongly Implicit Procedure For The Numerical Solution of Field Problems". Numerical Heat transfer, **4**, pp. 1-19.

Silveira Neto, A., 1991, "Simulation Numerique des Grandes Échelles d'un Écoulement Turbulent Décollé en Aval d'une Marche", Thèse de Doctorat, INPG, Grenoble, France.

Sinha, S. N., Gupta, A. K. e Oberai, M. M., 1982, "Laminar Separating Flow over Backsteps and Cavities. Part II: Cavities", AIAA Journal, **120**, 3, pp. 370-375.

Unverdi, S. O. e Tryggvason, G., 1992, "A Front-Tracking Method for Viscous Incompressible Multi-Fluid Flows", Journal of Computational Physics, **100**, pp. 25-60.